

Unusual electron-doping effects in $\text{Sr}_{2-x}\text{La}_x\text{FeMoO}_6$ observed by photoemission spectroscopy

T. Saitoh* and M. Nakatake†

Photon Factory, Institute of Materials Structure Science, KEK, Tsukuba, Ibaraki 305-0801, Japan

H. Nakajima‡ and O. Morimoto

Department of Materials Structure Science, Graduate University for Advanced Studies, Tsukuba, Ibaraki 305-0801, Japan

A. Kakizaki

Institute for Solid State Physics, University of Tokyo, Kashiwa, Chiba 277-8581, Japan

Sh. Xu and Y. Moritomo

Department of Applied Physics, Nagoya University, Nagoya 464-8603, Japan

N. Hamada

Department of Physics, Tokyo University of Science, Chiba 278-8510, Japan

Y. Aiura

National Institute of Advanced Industrial Science and Technology, Tsukuba, Ibaraki 305-8568, Japan

(Received 11 November 2004; revised manuscript received 10 March 2005; published 6 July 2005)

We have investigated the electronic structure of electron-doped $\text{Sr}_{2-x}\text{La}_x\text{FeMoO}_6$ ($x=0.0$ and 0.2) by photoemission spectroscopy and band-structure calculations within the local density approximation+ U scheme. A characteristic double-peak feature near the Fermi level (E_F) has been observed in the valence-band photoemission spectra of both $x=0.0$ and 0.2 samples. A photon-energy dependence of the spectra in the Mo $4d$ Cooper minimum region compared with the band-structure calculations has shown that the first peak crossing E_F consists of the (Fe+Mo) $t_{2g\downarrow}$ states (feature A) and the second peak well below E_F is dominated by the Fe $e_{g\uparrow}$ states (feature B). Upon La substitution, the feature A moves away from E_F by ~ 50 meV, which is smaller than the prediction of our band theory, 112 meV. In addition, an intensity enhancement of *both* A and B has been observed, although B does not cross E_F . Those two facts are apparently incompatible with the simple rigid-band shift due to electron doping. We point out that such phenomena can be understood in terms of the strong Hund's rule energy stabilization in the $3d^5$ configuration at the Fe sites in this compound. From an observed band-narrowing, we have also deduced a mass enhancement of ~ 2.5 with respect to the band theory, in good agreement with a specific heat measurement.

DOI: [10.1103/PhysRevB.72.045107](https://doi.org/10.1103/PhysRevB.72.045107)

PACS number(s): 79.60.-i, 71.20.Ps, 75.50.Gg

I. INTRODUCTION

Industrial demands on seeking new materials with exotic magnetotransport properties have been expanding the basic research field of transition-metal oxides with unusual magnetic and transport properties. Recent reinvestigations on the family of double perovskite-type oxides $A_2BB'O_6$ are one of such examples. The revived interest on the double perovskites has its origin in the large tunneling magnetoresistance discovered in $\text{Sr}_2\text{FeMoO}_6$ and $\text{Sr}_2\text{FeReO}_6$,^{1,2} although it had already been known since 1960s that $\text{Sr}_2\text{FeMoO}_6$ is a ferrimagnetic (or ferromagnetic) metal with a quite high ferrimagnetic transition temperature (T_C) of 420 K.³

Several band-structure calculations and optical or electron-spectroscopic studies have confirmed that those iron-based compounds generally have a half-metallic density of states (DOS) at the Fermi level (E_F).^{1,4-9} Ferrimagnetism accompanied by metallic conductivity and the half-metallic DOS naturally reminds us of the colossal magnetoresistive manganates and the double exchange (DE) mechanism. Indeed, several authors have pointed out that DE can explain the electronic properties of $\text{Sr}_2\text{FeMoO}_6$,⁸⁻¹¹ while others

have proposed a new mechanism of ferrimagnetic metal.^{12,13} Nevertheless, it is common in any models that the carrier density or DOS at E_F has much importance since the ferromagnetic interaction between Fe local spins is mediated by charge carriers (in DE models) or the Fe-O-Mo hybridized states (in hybridization models).

In this sense, a study of carrier-doping effects on the electronic structure of $\text{Sr}_2\text{FeMoO}_6$ is necessary to seek the origin of the ferrimagnetism of this compound. Navarro *et al.* have recently investigated this issue using polycrystalline samples of $\text{Sr}_{2-x}\text{La}_x\text{FeMoO}_6$.¹⁴ $\text{Sr}_{2-x}\text{La}_x\text{FeMoO}_6$ can be regarded as an electron-doped system of $\text{Sr}_2\text{FeMoO}_6$, where x corresponds to the number of doped electron per one Fe/Mo site. They have found that the E_F spectral weight linearly increases with x , in accordance with a linear increase of T_C . Although their result and argument seem to be clear and reasonable, there still remains an experimental and a theoretical concern: the former is about polycrystalline nature of their samples as well as the scratching surface treatment. In our previous paper,⁹ we have intensively discussed this issue and shown that spectra of $\text{Sr}_2\text{FeMoO}_6$ from a scraped and a fractured surface were quite different. In particular, the near-

E_F intensity was found to be considerably suppressed in scraping measurements. Since the near- E_F intensity is directly relevant to which model is plausible, a study using single crystals should be needed to address the above issue. In connection with theoretical studies, on the other hand, electron-doping effects should be examined first by band theory before we consider the DE or other new models. For example, if the calculated DOS is increasing monotonically with electron energy, the E_F DOS should linearly increase with x .

In this paper, we study the electron-doping effects on the electronic structure of single-crystalline $\text{Sr}_2\text{FeMoO}_6$ to give insight into the mechanism of ferrimagnetism and the half-metallic DOS by photoemission spectroscopy combined with local density approximation (LDA)+ U band-structure calculations. To avoid possible complications rising from a structural phase transition and antisite effects in heavily doped region¹⁵ and to probe only the electronic effects due to La substitution, we concentrate on a lightly doped region.

II. EXPERIMENT AND CALCULATION

High quality single crystals of $\text{Sr}_{2-x}\text{La}_x\text{FeMoO}_6$ ($x=0.0$ and 0.2) were grown by floating-zone method.⁴ The site disorder was about 10%–15% which lowers the T_C from the ideal values,¹⁶ but will not seriously affect the microscopic electronic structure.⁹ The experiments have been performed at the beamline BL-11D of the Photon Factory using a Scienta SES-200 electron analyzer. The total energy resolution was about 50–90 meV full width at half maximum using 65–200 eV photon energies. The vacuum was always better than 1.5×10^{-10} Torr and the temperature was about 20 K. To obtain the best quality of surface, we have fractured samples *in situ* at 20 K. The prepared surface was blackly shining like a cleaved surface, but was rough enough to obtain angle-integrated spectra, although angle-resolved effects appeared in low photon energies to some extent. For comparison, we have also scraped samples with a diamond file.⁹ The spectral intensity was normalized by the total area of the full valence-band spectra and the near- E_F spectra were scaled to them.

Band-structure calculations for nondoped $\text{Sr}_2\text{FeMoO}_6$ have been performed with the full-potential linearized augmented plane-wave method within the LDA+ U scheme. For effective Coulomb repulsions $U_{\text{eff}}=U-J$, we have adopted rather small values (2.0 eV for Fe and 1.0 eV for Mo). More detailed information is given in Ref. 9.

III. RESULTS AND DISCUSSION

Figure 1 shows photoemission spectra of the valence band of $\text{Sr}_{2-x}\text{La}_x\text{FeMoO}_6$ with shallow core levels at 20 K. A doublet structure at -19.1 and -20.0 eV is the Sr $4p$ core level, which is on the long tail of the O $2s$ core level at -22.1 eV. Upon La substitution, another doublet structure due to the La $5p$ core level appears at -17.4 and -19.6 eV. However, it is very weak due to a small photoionization cross section.¹⁷ The strong enhancement of the La $5p$ intensity at $h\nu = 120$ eV is attributed to the La $4d-4f$ giant resonance.¹⁸ A

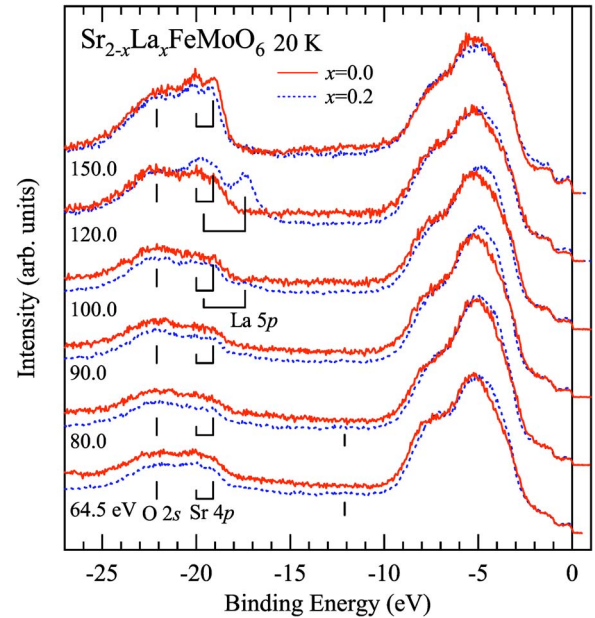


FIG. 1. (Color online) Photoemission spectra of the valence band with shallow core levels of $\text{Sr}_{2-x}\text{La}_x\text{FeMoO}_6$ at 20 K.

very small structure at 12.1 eV observed in lower photon-energy spectra is most likely due to surface aging effects.

Figure 2 shows full valence-band spectra of $\text{Sr}_{2-x}\text{La}_x\text{FeMoO}_6$ at 20 K. One can observe six structures denoted as A to F. A comparison with the band-structure calculations clarifies that the double-peak structures A and B near E_F correspond to the (Fe+Mo) $t_{2g\downarrow}$ and Fe $e_{g\uparrow}$ bands,

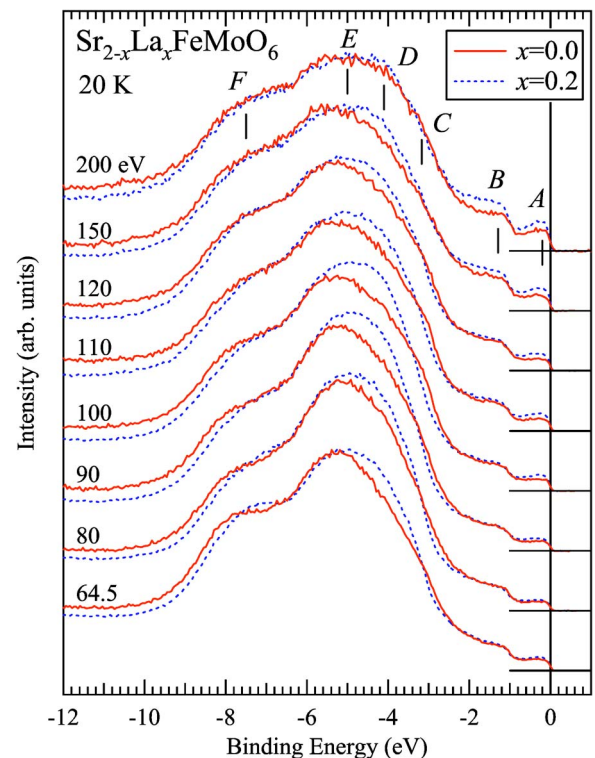


FIG. 2. (Color online) Valence-band photoemission spectra of $\text{Sr}_{2-x}\text{La}_x\text{FeMoO}_6$ at 20 K.

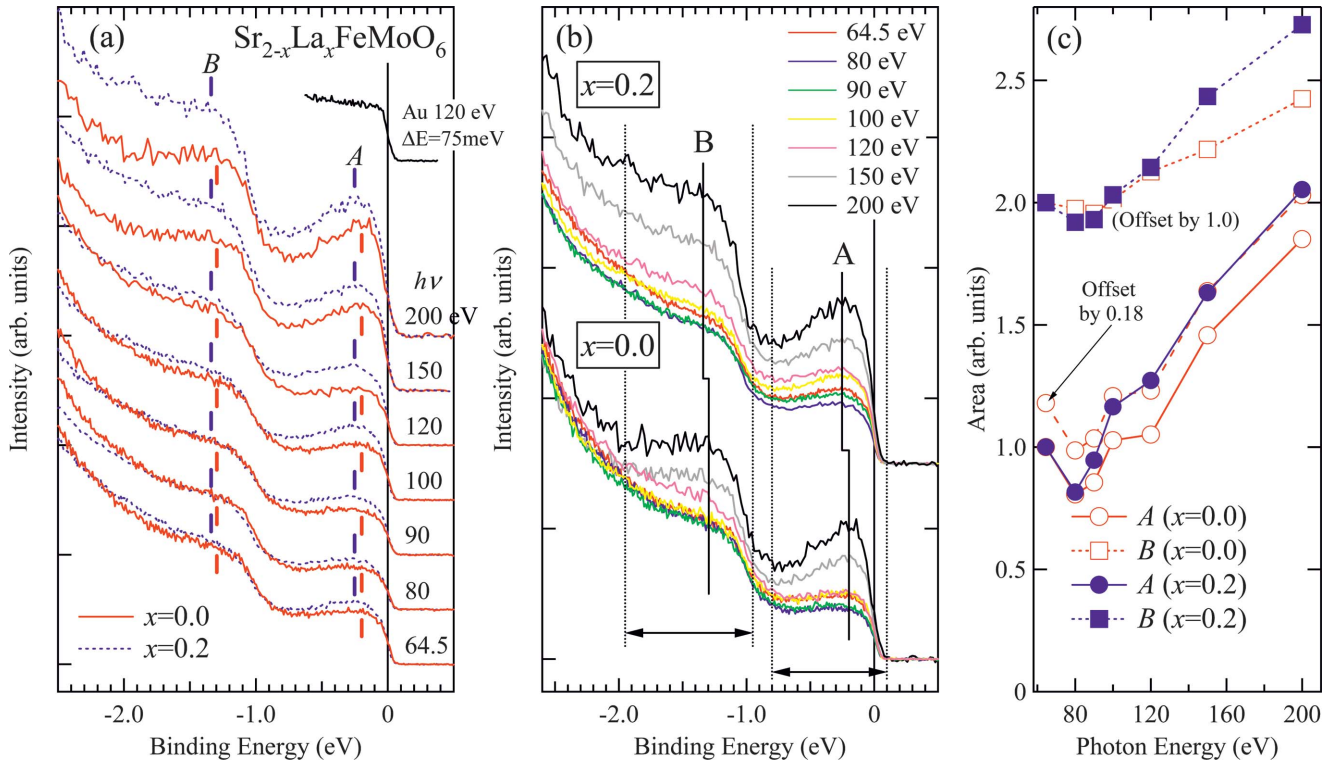


FIG. 3. (Color) (a) Near- E_F photoemission spectra of $\text{Sr}_{2-x}\text{La}_x\text{FeMoO}_6$ at $T=20$ K. Red ($x=0.0$) and blue ($x=0.2$) bars indicate the locations of features A and B. A gold spectrum at 120 eV is also shown. (b) Photon-energy dependence of the $x=0.0$ and the $x=0.2$ near- E_F spectra. The data are same as in (a). (c) Normalized spectral weights of A and B calculated using windows of -0.8 to 0.1 eV (A) and -1.95 to -0.95 eV (B). The windows are indicated in Panel (b). The spectral weight at 64.5 eV is set to unity. Note that the weight for B includes an offset of 1.0.

respectively.^{1,6-9,11,12} In addition, C and D originate mostly from the Fe $t_{2g\uparrow}$ bands with a contribution from the O $2p$ intensity. E is predominantly due to the O $2p$ nonbonding states. The Fe $t_{2g\uparrow}$ and $e_{g\uparrow}$ bonding states contribute to F to some extent. The features D and E are somewhat enhanced in the low-photon-energy spectra upon La substitution. This can be interpreted primarily as angle-resolved effects because the enhancement becomes small with increasing photon energy and almost vanishes for all C–F at the highest 200 eV spectrum.

By contrast, substantial changes are observed in the near- E_F region of all the spectra as shown in Fig. 3. Panel (a) of Fig. 3 shows near- E_F spectra of $\text{Sr}_{2-x}\text{La}_x\text{FeMoO}_6$. Upon La substitution, the features A and B are shifted from -0.20 to -0.25 eV and from -1.30 to -1.34 eV, respectively. Although the direction of the shift is in accordance with electron doping, the amount of the shift (~ 40 – 50 meV)¹⁹ is too small; Figure 4 illustrates the expected location of E_F deduced from our LDA+ U band-structure calculation assuming the rigid band shift. It predicts that $x=0.2$ (0.2 electron doping per one Fe/Mo site) should correspond to a E_F shift of 112 meV while the 50 meV shift of E_F corresponds to $x=0.086$.

Panel (b) of Fig. 3 shows a photon-energy dependence of the near- E_F spectra. The intensity of the features A and B tends to increase with $h\nu$, indicating that considerable Fe $3d$ weight compared to the O $2p$ one exists in those features.¹⁷ However, one can notice that the intensity at A does not

increase monotonically but has a minimum at ~ 80 eV, while such a clear minimum is not observed in B. This is because the Cooper minimum of Mo $4d$ states strongly suppresses the Mo $4d$ weight around ~ 80 – 90 eV and only the feature A has a substantial contribution from Mo $4d$ states.^{9,17}

These behaviors of the spectral weight of A and B versus $h\nu$ are summarized in panel (c). Panel (c) shows a normalized spectral weight of A and B. Here we set the 64.5 eV to unity as a reference. A clear minimum around 80 eV for the feature A is attributed to the Cooper minimum of Mo $4d$

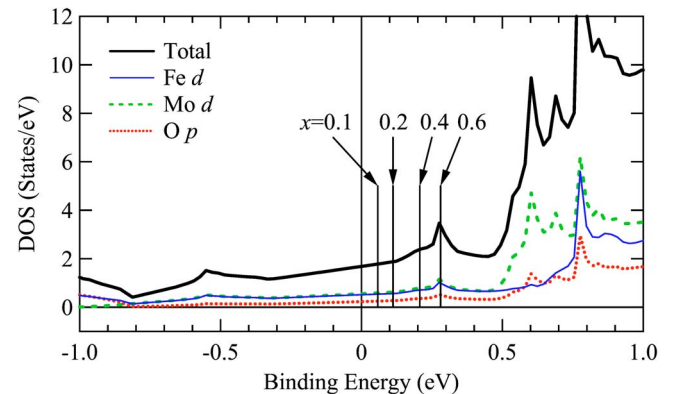


FIG. 4. (Color online) Total and partial DOS of $\text{Sr}_2\text{FeMoO}_6$ in the near- E_F region calculated by the LDA+ U method. Vertical lines denote expected locations of E_F deduced from the calculation, assuming the rigid band shift due to electron doping.

states. The Cooper minimum is obviously enhanced in the $x=0.2$ curve, while the two curves are virtually parallel to each other above the minimum. This observation indicates that the Mo $4d$ contribution to the feature A is larger for $x=0.2$ than $x=0.0$, but no significant change in the Fe $3d$ and O $2p$ contributions. Namely, the doped electrons are introduced mainly into the Mo $4d t_{2g}$ states, as inferred by Moritomo *et al.*⁴ More recently, Frontera *et al.* have observed by neutron diffraction that the Mo—O distance increases with La doping while the Fe—O one does not change.²⁰ In terms of the ionic-radius argument, this implies that the doped electrons will be located mainly at the Mo sites,²⁰ in agreement with the above argument. On the other hand, the spectral weight at the feature B of $x=0.2$ is also considerably enhanced in the high photon energies despite the fact that the two curves are virtually identical below 120 eV. This indicates that the feature B (Fe $e_{g\uparrow}$ bands) also obtains electrons. However, it cannot be a simple consequence of electron doping because the feature B is not crossing over E_F owing to the half-metallic DOS.

Such an unusual behavior, the enhancement of *both* A and B due to electron doping, has also been reported in the recent photoemission study on polycrystalline samples by Navarro *et al.*¹⁴ The fact that two independent experiments using different samples with different surface treatments have given the same result apparently demonstrates that this is an intrinsic change of the electronic structure due to electron doping. This is of course not of the rigid-band type, but also incompatible with the behavior of typical electron- or hole-doped $3d$ transition-metal oxides such as $\text{La}_{1-x}\text{Sr}_x\text{TiO}_3$ or $\text{La}_{1-x}\text{Sr}_x\text{MnO}_3$. In these compounds, in-gap states induced by carrier doping always appear between the top of the valence band and the bottom of the conduction band and are crossing E_F .^{21–24}

We believe that the above strange behavior can be understood in terms of the strong Hund's rule coupling in the Fe d^5 configuration as follows: the electron configuration in $\text{Sr}_2\text{FeMoO}_6$ is not completely $[3d^5+4d^1]$ -like,²⁵ but still has some weight of the $[3d^5\bar{L}(e_g)+4d^2]$ configuration in which $3d^5\bar{L}(e_g)$ is the dominant electron configuration in the "original" SrFeO_3 -like environment for Fe ions.⁹ Here, \bar{L} denotes an O $2p$ ligand hole. Upon electron doping, the electron configuration will be changing from either $[3d^5+4d^1]$ or $[3d^5\bar{L}(e_g)+4d^2]$ configuration to be more like a $[3d^5+4d^2]$ configuration because the strong Hund's rule energy stabilization of the d^5 configuration prevents the Fe sites from having more than five electrons.⁹ As a consequence, the doped electrons will occupy either Mo $4d$ states or ligand-hole states, resulting in the enhancement of both features A (Mo $4d$ states) and B (Fe $3d e_g$ states).²⁶ The enhancement in the feature B due to electron doping thus reflects the strong Hund's rule energy stabilization in this compound.

Figure 5 shows a comparison between experimental and theoretical E_F spectral weight plotted as functions of La concentration x . The photoionization cross sections are taken into account for theoretical curves. The theoretical E_F weight increases almost linearly with x . Here, the 50 and 200 eV curves predominantly represent both Fe $3d$ and Mo $4d$ weight, and the 90 eV should represent only the Fe $3d$

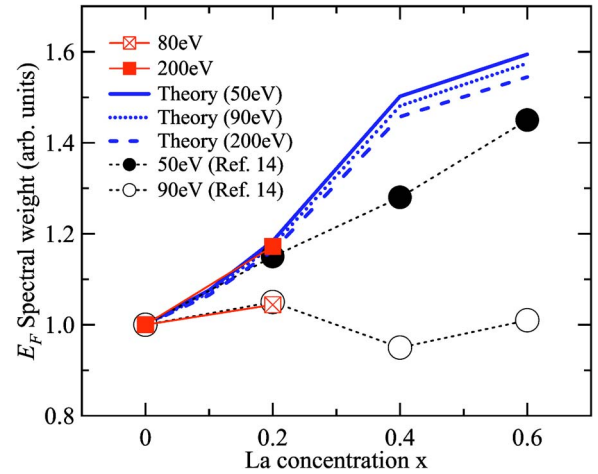


FIG. 5. (Color online) Experimental and theoretical E_F spectral weights plotted as functions of La concentration x . The E_F spectral weight was evaluated from integration within a ± 0.1 eV window at E_F and normalized with respect to the $x=0.0$ one. The rigid-band shift is assumed in the theoretical curves and the photoionization cross sections of Fe $3d$, Mo $4d$, and O $2p$ states are taken into account. Results by Navarro *et al.* (Ref. 14) are also shown for comparison.

weight.²⁷ It is noted that all the three theoretical curves have no significant difference although the 90 eV curve would have smaller weight due to the Mo $4d$ Cooper minimum. This comes from the small Mo $4d$ DOS due to the high valence of Mo ions. Nevertheless, the experimental E_F weight for 80 and 200 eV displays a considerable difference. Here it is worthy to note that our 200 and 80 eV curves are almost identical to the 50 and 90 eV ones by Navarro *et al.*, respectively.²⁸ On the other hand, they have reported a linear relationship between the E_F spectral weight and T_C (see Fig. 5).¹⁴ One may consider that it can be evidence of the DE mechanism in this compound, although they carefully mentioned that there were several possibilities. In our measurements, T_C is not enhanced upon electron doping⁴ due to the site disorder.¹⁶ It is noted, however, that the observed E_F spectral weight is almost identical to their results. Therefore, we infer that the enhancement of the E_F weight in both experiments may not be a direct consequence of the DE mechanism although we also believe that the DE mechanism can basically describe the electronic structure of this compound.⁹

The discrepancy between theory and experiment in the Cooper minimum region possibly indicates that the Mo $4d$ states have larger near- E_F weight than expected from the band theory. This does not necessarily mean that more Mo $4d$ electrons nominally exist but the O $2p$ and Fe $3d t_{2g\downarrow}$ states, which strongly hybridize with Mo $4d t_{2g\downarrow}$ ones, may be able to contribute to the Mo $4d$ spectral weight to some extent. This argument can also explain a small (a factor of 1.5) suppression of the intensity at the feature A in an experimental spectrum compared with a band-theory simulation shown in Fig. 5 of Ref. 9. However, it would be inconsistent with Mössbauer measurements which concluded $\text{Fe}^{2.5+}$.^{29,30} Hence, this discrepancy is an open question at this stage.

On the other hand, both our 200 eV curve and the 50 eV curve by Navarro *et al.* coincide with the theoretical ones up

TABLE I. LDA+ U band DOS at E_F $N_B(E_F)$ (in 10^{24} eV $^{-1}$ mol $^{-1}$), electronic specific heat γ_B deduced from $N_B(E_F)$ [in mJ/(K 2 mol)], a mass enhancement estimated from the electronic specific heat $\gamma_{\text{exp}}/\gamma_B$, and a mass enhancement estimated from the band-narrowing W_{exp}/W_B .

x	0.0	0.1	0.2	0.4	0.6
$N_B(E_F)^a$	1.0	1.1	1.1	1.4	1.9
γ_B	4.0	4.2	4.4	5.6	7.5
γ_{exp}^b	10	10	12		
$\gamma_{\text{exp}}/\gamma_B$	2.5	2.4	2.7		
W_{exp}/W_B	2.5		2.2–2.8		

^aRigid-band shift is assumed for $x > 0$.

^bTaken from Ref. 4.

to $x=0.2$. Because we set all the spectral weights for $x=0.0$ to unity as a reference, this implies $W_{\text{exp}}(0.2)/W_{\text{exp}}(0.0) \approx W_B(0.2)/W_B(0.0)$, where W_{exp} and W_B denote the experimental and theoretical spectral weights at E_F , respectively. However, this is not a consequence of the rigid-band shift, as we have presented above. Instead, this situation can be realized if a band-narrowing occurs uniformly in the (Fe+Mo) $t_{2g\downarrow}$ band. We believe that such a band-narrowing is realized since the system is a good metal. In $\text{La}_{1-x}\text{Sr}_x\text{TiO}_{3+y/2}$ case, for example, this type of narrowing appears in the Fermi liquid phase, whereas a narrowing occurs only in the vicinity of E_F when the system is close to the metal-insulator transition.³¹

Based upon the uniform band-narrowing assumption, the ratio of the theoretical chemical potential shift to that of the experiment should represent the mass enhancement from the band mass. In Table I, two estimations of mass enhancement $\gamma_{\text{exp}}/\gamma_B$ and W_{exp}/W_B are listed. A theoretical electronic specific heat γ_B is deduced from the band-theory DOS at E_F [$N_B(E_F)$] using the formula $\gamma_B = \pi^2 k_B^2 N_B(E_F)/3$. W_{exp}/W_B describes a mass enhancement estimated from the band-narrowing. For $x=0.0$, this number is deduced from the location of the feature A (theory: -0.50 eV, experiment: -0.20 eV)⁹ and for $x=0.2$, we make use of the ratio of the chemical potential shift (theory: 112 meV, experiment: 40–50 meV) based on the above argument. They give W_{exp}/W_B of 2.5 ($x=0.0$) and 2.2–2.8 ($x=0.2$), in good agreement with the estimation from γ_{exp} . Therefore, electron-doping effects on the (Fe+Mo) $t_{2g\downarrow}$ band can be understood in terms of a conventional electron doping into a renormalized (by a factor of two) band like the $\text{La}_{1-x}\text{Sr}_x\text{TiO}_3$ case.^{31,32} Currently, we have no idea to determine how many electrons will be introduced into the Mo(+Fe) $t_{2g\downarrow}$ band and the Fe $e_{g\uparrow}$ band, respectively, in our scenario of electron doping, $\alpha|3d^5 4d^1\rangle + \beta|3d^5 \underline{L}(e_g) 4d^2\rangle \rightarrow |3d^5 4d^2\rangle$ ($|\alpha| \gg |\beta|$). However,

it is safe to say that the doping effects should appear in the feature A more than in the feature B because $|\alpha| \gg |\beta|$. In this sense, the observed enhancement in the feature A is rather smaller than expected. This can be understood again in connection with the small photoionization cross section of the Mo 4d states, if we assume that the electrons doped into the (Fe+Mo) $t_{2g\downarrow}$ band will mostly occupy the Mo 4d states.

IV. CONCLUSION

We have investigated the electronic structure of $\text{Sr}_{2-x}\text{La}_x\text{FeMoO}_6$ by photoemission spectroscopy and LDA+ U band-structure calculations. A double-peak structure observed at about -0.2 eV (feature A) and -1.3 eV (feature B) was identified to be a Fe+Mo $t_{2g\downarrow}$ band and a Fe $e_{g\uparrow}$ band, respectively. The chemical potential shift due to electron doping was observed to be about 40–50 meV which was considerably smaller than the prediction of the band theory, 112 meV. In addition, the features A and B were both enhanced due to electron doping. We have pointed out that this unusual enhancement at the feature B is probably indicating a characteristic distribution of doped electrons triggered by the strong Hund's rule energy stabilization in the $3d^5$ configuration. From the observed band-narrowing, we have deduced a mass enhancement of ~ 2.5 with respect to the band theory, which is in good agreement with a specific heat measurement.

ACKNOWLEDGMENTS

The authors would like to thank T. Kikuchi for technical support in the experiment. The experimental work has been done under the approval of the Photon Factory Program Advisory Committee (Proposal No. 00G011). This work was supported by a Grant-in-Aid for Scientific Research from the Japanese Ministry of Education, Culture, Sports, Science, and Technology.

*Present address: Department of Applied Physics, Tokyo University of Science, Shinjuku-ku, Tokyo 162-8601, Japan; electronic address: t-saitoh@rs.kagu.tus.ac.jp

[†]Present address: Hiroshima Synchrotron Radiation Center, Hi-

roshima University, Higashi-Hiroshima, Hiroshima 739-8521, Japan.

[‡]Present address: National Synchrotron Research Center, PO Box 93, Nakhon-Ratchasima 30000, Thailand.

- ¹K.-I. Kobayashi, T. Kimura, H. Sawada, K. Terakura, and Y. Tokura, *Nature (London)* **395**, 677 (1998).
- ²K.-I. Kobayashi, T. Kimura, Y. Tomioka, H. Sawada, K. Terakura, and Y. Tokura, *Phys. Rev. B* **59**, 11159 (1999).
- ³F. Galasso, F. C. Douglas, and R. Kasper, *J. Chem. Phys.* **44**, 1672 (1966).
- ⁴Y. Moritomo, Sh. Xu, T. Akimoto, A. Machida, N. Hamada, K. Ohoyama, E. Nishibori, M. Takata, and M. Sakata, *Phys. Rev. B* **62**, 14224 (2000).
- ⁵Y. Tomioka, T. Okuda, Y. Okimoto, R. Kumai, K.-I. Kobayashi, and Y. Tokura, *Phys. Rev. B* **61**, 422 (2000).
- ⁶Z. Fang, K. Terakura, and J. Kanamori, *Phys. Rev. B* **63**, 180407(R) (2001).
- ⁷H. Wu, *Phys. Rev. B* **64**, 125126 (2001).
- ⁸J.-S. Kang, H. Han, B. W. Lee, C. G. Olson, S. W. Han, K. H. Kim, J. I. Jeong, J. H. Park, and B. I. Min, *Phys. Rev. B* **64**, 024429 (2001).
- ⁹T. Saitoh, M. Nakatake, A. Kakizaki, H. Nakajima, O. Morimoto, Sh. Xu, Y. Moritomo, N. Hamada, and Y. Aiura, *Phys. Rev. B* **66**, 035112 (2002).
- ¹⁰B. Martínez, J. Navarro, Ll. Balcells, and J. Fontcuberta, *J. Phys.: Condens. Matter* **12**, 10515 (2000).
- ¹¹Y. Moritomo, Sh. Xu, A. Machida, T. Akimoto, E. Nishibori, M. Takata, and M. Sakata, *Phys. Rev. B* **61**, R7827 (2000).
- ¹²D. D. Sarma, P. Mahadevan, T. Saha-Dasgupta, S. Ray, and A. Kumar, *Phys. Rev. Lett.* **85**, 2549 (2000).
- ¹³J. Kanamori and K. Terakura, *J. Phys. Soc. Jpn.* **70**, 1433 (2001).
- ¹⁴J. Navarro, J. Fontcuberta, M. Izquierdo, J. Avila, and M. C. Asensio, *Phys. Rev. B* **69**, 115101 (2004).
- ¹⁵J. Navarro, C. Frontera, Ll. Balcells, B. Martínez, and J. Fontcuberta, *Phys. Rev. B* **64**, 092411 (2001).
- ¹⁶Y. Moritomo, N. Shimamoto, Sh. Xu, A. Machida, E. Nishibori, M. Takata, M. Sakata, and A. Nakamura, *Jpn. J. Appl. Phys., Part 2* **40**, L672 (2001).
- ¹⁷J. J. Yeh and I. Lindau, *At. Data Nucl. Data Tables* **32**, 1 (1985).
- ¹⁸For example, S. L. Molodtsov, Yu. Kucherenko, J. J. Hinarejos, S. Danzenbächer, V. D. P. Servedio, M. Richter, and C. Laubschat, *Phys. Rev. B* **60**, 16435 (1999).
- ¹⁹The accuracy of the location of *A* was ± 10 meV but that of *B* was much worse due to the broader feature. Thus, we have also estimated the shift of the spectra using the steep edge between the features *A* and *B*, with accuracy of ± 5 meV.
- ²⁰C. Frontera, D. Rubi, J. Navarro, J. L. García-Muñoz, J. Fontcuberta, and C. Ritter, *Phys. Rev. B* **68**, 012412 (2003).
- ²¹A. Fujimori *et al.*, *Phys. Rev. B* **46**, R9841 (1992).
- ²²K. Morikawa, T. Mizokawa, A. Fujimori, Y. Taguchi, and Y. Tokura, *Phys. Rev. B* **54**, 8446 (1996).
- ²³T. Saitoh, A. E. Bocquet, T. Mizokawa, H. Namatame, A. Fujimori, M. Abbate, Y. Takeda, and M. Takano, *Phys. Rev. B* **51**, 13942 (1995).
- ²⁴J.-H. Park, C. T. Chen, S.-W. Cheong, W. Bao, G. Meigs, V. Chakarian, and Y. U. Idzerda, *Phys. Rev. Lett.* **76**, 4215 (1996).
- ²⁵We note that the expression $[3d^5+4d^1]$ is a simplified description. A more realistic expression is $[3d^{5+\delta}+4d^{1-\delta}]$ ($\delta \sim 0.5$) because Mössbauer measurements have concluded $\text{Fe}^{2.5+}$ (Refs. 29 and 30). However, this does not mean that the $[3d^5+4d^1]$ configuration does not exist at all; in terms of the local configuration-interaction description (around the Fe sites), $[3d^5+4d^1]$ still has a major weight and $[3d^6\bar{L}+4d^1]$, $[3d^6+4d^0]$, and $[3d^5\bar{L}+4d^2]$, etc. have some weight, respectively. This is one of the reasons that the nominal valences of Fe and Mo are often written as 3+ and 5+, respectively (in spite of the Mössbauer measurements). Thus, we have used the major configuration $[3d^5+4d^1]$ for simplicity.
- ²⁶If we assume that doped electrons may occupy the Fe 3*d* states, Fe t_{2g} states (namely, the feature *A*), should be enhanced due to electron doping and no enhancement would be observed at the feature *B*. This consideration further reinforces our argument.
- ²⁷We note that the 80 eV curve is not shown because it is indistinguishable from the 90 eV curve.
- ²⁸In our measurements, the spectra are suppressed most at 80 eV, while Navarro *et al.* have adopted 90 eV.
- ²⁹J. Lindén, T. Yamamoto, M. Karppinen, H. Yamauchi, and T. Pietari, *Appl. Phys. Lett.* **76**, 2925 (2000).
- ³⁰S. Nakamura, K. Ikezaki, N. Nakagawa, Y. J. Shan, and M. Tanaka, *Hyperfine Interact.* **141–142**, 207 (2002).
- ³¹T. Yoshida, A. Ino, T. Mizokawa, A. Fujimori, Y. Taguchi, T. Katsufuji, and Y. Tokura, *Europhys. Lett.* **59**, 258 (2002).
- ³²Y. Tokura, Y. Taguchi, Y. Okada, Y. Fujishima, T. Arima, K. Kumagai, and Y. Iye, *Phys. Rev. Lett.* **70**, 2126 (1993).